Comparison of Results Between the Miniature FASat-Bravo Ozone Mapping Detector (OMAD) and NASA's Total Ozone Mapping Spectrometer (TOMS)

Juan A. Fernandez-Saldivar, Craig I. Underwood
Surrey Space Centre, University of Surrey
GU2 7XH, United Kingdom; Phone: +44 (0)1483 689809
c.underwood@surrey.ac.uk; j.fernandez@surrey.ac.uk

ABSTRACT

The Ozone Layer Monitoring Experiment (OLME) on board the FASat-Bravo microsatellite launched in July 1992 observed backscattered UV to retrieve atmospheric ozone using two instruments: the Ozone Ultraviolet Backscatter Imager (OUBI) and the Ozone Mapping Detector (OMAD). Initial results from this experiment have shown good qualitative agreement with data from NASA's TOMS instrument [1]. More recent studies of OMAD data have found quantitative agreement in their radiances and even indicated detection of a volcanic eruption plume from the Nyamuragira volcano [2].

INTRODUCTION

Typically, monitoring of the atmosphere in the UV from space has been exclusive to large platforms. In the visible spectrum constellations of small satellites have proven to be a success for disaster monitoring and earth observation applications using multi-spectral capabilities. Hyperspectral capabilities have also been applied in the visible and Near Infrared from 400-1050 nm in land and ocean applications from Compact High Resolution Imaging Spectrometer (CHRIS) on-board small satellite PROBA. In the literature, few proposals and examples of the efficacy of micro-satellite instrumentation using the UV range of the solar spectrum have been reported.

The Ozone Layer Monitoring Experiment (OLME) on-board the 50 kg FASat-Bravo microsatellite was launched in July 1998 into an 820 km altitude, sun-synchronous orbit. The aim of this experiment was to study ozone (O_3) concentrations in the Antarctic region with special attention to the Chilean territory and comprised two low-cost instruments: the Ozone Ultraviolet Backscatter Imagers (OUBI) using a UV-coated CCD and the Ozone Mapping Detector (OMAD) based on silicon photodiodes

Ozone Mapping Detector (OMAD)

OMAD is a 4-channel radiometer with 10-nm resolution bands at 289, 313, 334 and 380 nm [1], working continuously with a Field of View (FOV) of 11° x 11° providing a ground resolution of 150 x 150 km. It used a single fused silica lens AR coated on all four channels with focal length 12.5 mm and F-number 1.1.

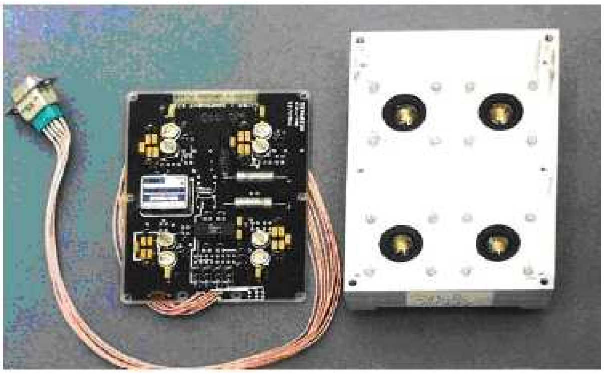

Figure 1 Ozone Mapping Detector (OMAD)

A silicon detector for each channel with a sensitive area of 2.4 x 2.4 mm^2 provided 12-bit photocurrent resolution drawing only 500 mW when in operation [1].

The power consumption of the OMAD payload was sufficiently low that the payload was left powered on continuously, thus mapping the Earth and atmosphere from its nadir-pointing position on the base-plate of the FASat-Bravo microsatellite. The data were recorded by the On-Board Computer (OBC) and downloaded each day.

Table 1: OMAD Channel Specifications [1]

Channel [nm]	Gain [VA^{-1}]	Responsivity [AW^{-1}]	Total Nominal Transmission factors	Measured Bandwidth [nm]
289	1.00E+10	0.13	0.422	9.5
313	4.13E+07	0.14	0.734	9.4
334	5.40E+06	0.15	0.719	10.3
380	4.13E+07	0.18	0.147	10

OMAD channels were chosen to be processed in a ratio of channels at 313 nm and 334 nm to derive total column ozone content as these channels correspond to the ozone backscatter UV spectrum absorption band. A longer wavelength channel at 380 nm (corresponding to UV albedo) is taken as a reference for the particular reflectance conditions of the scene as high albedos (e.g. from clouds) can confuse the ozone retrieval algorithm.

Details of the algorithm developed to retrieve total column ozone content are given next:

OMAD OZONE ALGORITHM

The new algorithm uses empirical factors to derive and restrict the reflectance conditions under which the algorithm should operate, thus ignoring cloud fractions above a threshold, to minimise retrieval errors. These factors are derived from TOMS-Level2 version 8 products through vicarious calibration once the data has been gridded to a common latitude/longitude reference grid. It also uses a geometrical Air Mass Factor (AMF) based on observing conditions to obtain the vertical column content from the slant column amount derived from the initial simplified algorithm.

The un-calibrated slant column amount is derived from the initial simplified algorithm based on the estimated radiance from the two "ozone" channels (L_{334} and L_{313}).

$$uO3_{slant} = \text{Log}\,(L_{334} / L_{313}) \qquad (1)$$

It is then corrected using a Geometrical Air Mass Factor (GAMF) based on the solar zenith angle (θ) given the observing conditions defined as:

$$GAMF = 1 / \cos(\theta) \qquad (2)$$

From (1) and (2), we obtain a representative value of the vertical ozone content $OMAD_{O3}$.

$$OMAD_{O3} = uO3_{slant} - \text{Log}\,(GAMF) \qquad (3)$$

In order to obtain the real vertical column content from (3) we used an empirical linear function based on geographical zones

$$O3_{vertical} = M_{zone} \times OMAD_{O3} + B_{zone} \qquad (4)$$

Where, M_{zone} is the empirical slope factor for a given zone and B_{zone} is the empirical intercept factor for a given zone.

These two empirical factors allow us to account for various aspects: the most important is due to variations in ozone profiles that normally change with latitude; atmospheric profiles of temperature and pressure also vary with geography and continental/ocean masses. Other aspects include: the different spectral resolution of OMAD, (10 times wider than NASA's Total Ozone Mapping Spectrometer – TOMS-EP) and its ground sample area (also 10 times larger than TOMS) and the viewing geometry affecting the air mass factor (nadir only vs across track scan).

A geographical overview of the empirical parameters is shown next:

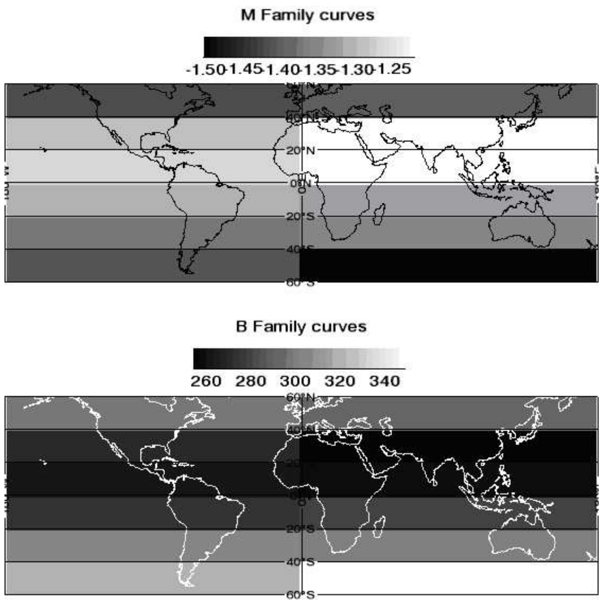

Figure 2: Empirical Parameters by Zone

These factors were derived by a curve-fitting and residual error minimization technique using NASA TOMS derived ozone concentration data as the "ground-truth".

Figure 3 shows the effect of using an appropriate and arbitrary pair of parameters (M, B).

The "true" O_3 content derived from TOMS data is shown in black; the OMAD equivalent using an arbitrary pair of empirical factors (actually those for the equatorial zone 8) is shown in green, and the appropriate region-based empirical parameter corrected OMAD data is shown in blue.

This shows that a single pair of parameters derived (say) from OMAD data gathered in the tropical regions would overestimate the ozone content at other regions. However, the region-corrected empirical parameters give a much better fit to the NASA TOMS data.

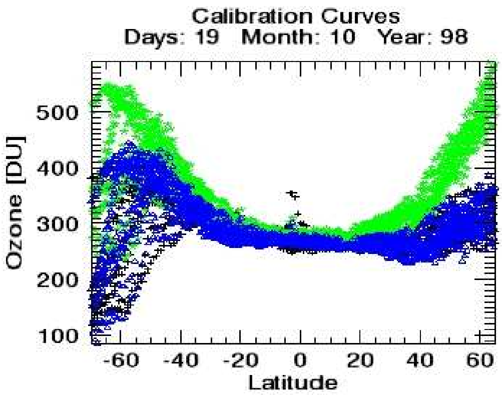

Figure 3: Different Calibration Curves for OMAD O_3 Data (Blue, Green) vs TOMS O_3 Data (Black).

The anomalous peak seen in the TOMS data near zero latitude was caused by the Nyamuragira volcanic eruption and it is only present for data taken on the 19th October 1998.

This signal is not actually caused by ozone, but instead is due to a very large concentration of sulphur dioxide (SO_2) that was present in the upper atmosphere due to the volcanic plume resulting from the eruption. SO_2 has a strong absorption feature in the UV virtually coincident with that due to ozone. The peak is not as clear in the OMAD data due to the wider spectral response of the OMAD channels.

To fully calibrate the OMAD data, the M and B parameters were derived for all regions and all days for the dataset analysed. The temporal and regional variations of these parameters are represented in the contour plots shown below (Figure 4). Whilst there is some variation in the parameters day-to-day within a particular region (which may be related to the changing nature of the cloudscape day by day) – it is the regional differences which show up most sharply.

The lowest M parameters (~100) are centred just north of the equator (regions 5 and 6). They reach a maximum of (~400) in the southernmost regions 11 and 12. This would lead to a rather large variation in slope (M) if we did not take into account that the intercept (B) parameter behaves somewhat inversely having the lowest values (~ -200) in the southernmost regions. This is partly due to the fitting method resulting in certain coupling between M and B.

Once the appropriate M and B parameters are determined, "calibrated" OMAD ozone results (measured in Dobson Units [DU]) can be derived. Figure 5 shows that the fit to NASA TOMS data is now good and the low ozone values normally expected during the austral spring are clearly observed.

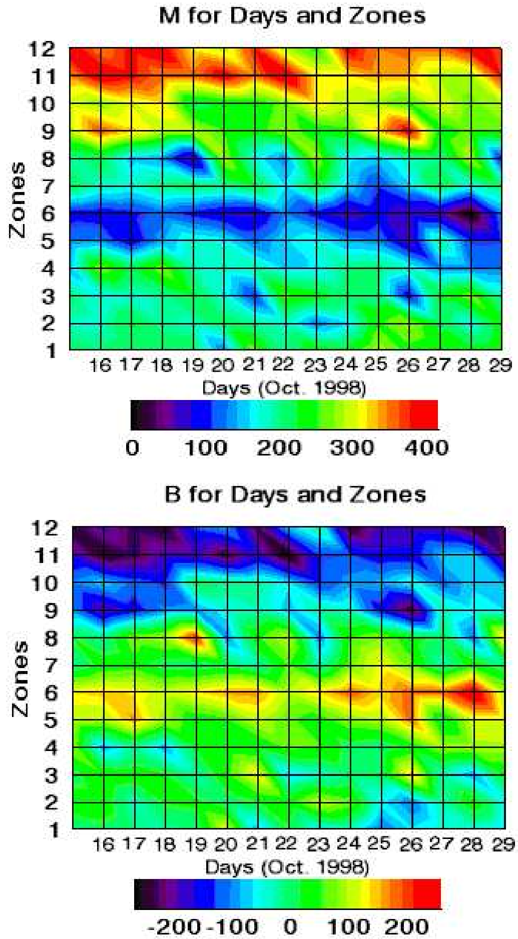

Figure 4: Empirical M and B Parameters

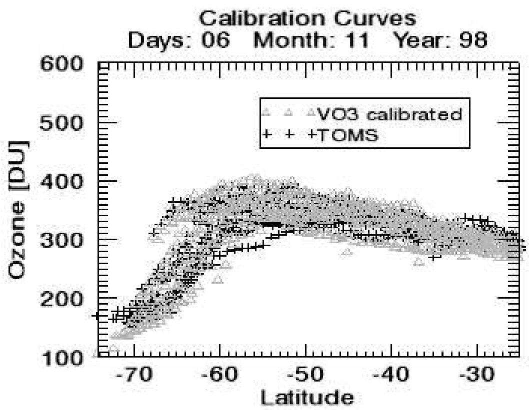

Figure 5: Total Ozone vs Latitude for OMAD and TOMS

The differences between OMAD and TOMS observations are greater at lowest latitudes. This is due the non-linearity of the air mass factors encountered at these latitudes and their longitudinal variability as the ozone hole develops.

The relative error between OMAD and TOMS data with respect to the total ozone content derived using TOMS v.8.0. is shown below:

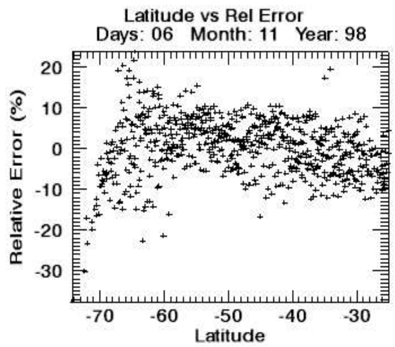

Figure 6: Relative Error in Total Ozone Content Derived from Comparison of TOMS and OMAD Data Using this Calibration Method.

Even after the regional calibration has been applied, the relative errors of southern latitudes are generally larger than those of equatorial regions. Relative errors of less than 10% are obtained above ~60 degrees in latitude.

Throughout the period under analysis the correlation between the TOMS and OMAD products is maintained high (Figure 7). We believe the relative error can be explained by extreme viewing geometries, different timing and differences in ground sample distances for the two instruments: the spectral resolution of OMAD is 10 times wider and its ground sample area is 10 times larger than that of TOMS; orbital differences also imply different timing between overpasses and viewing conditions (OMAD is nadir-viewing only, whilst TOMS scans across-track). The results obtained are in good agreement overall despite these inherent instrumental differences.

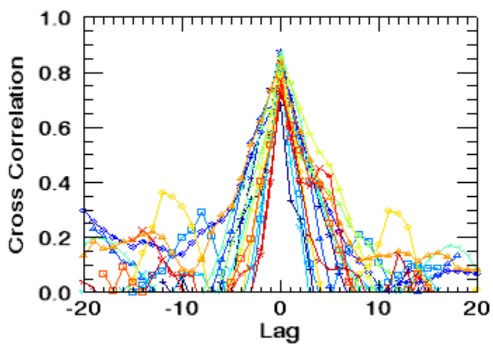

Figure 7: Cross Correlation OMAD vs TOMS Total Ozone Column

A visual indication of the level of agreement in all regional zones is clear from their final products. A single day of a TOMS's data mapped to its ground track is shown in Figure 8, together with the OMAD equivalent.

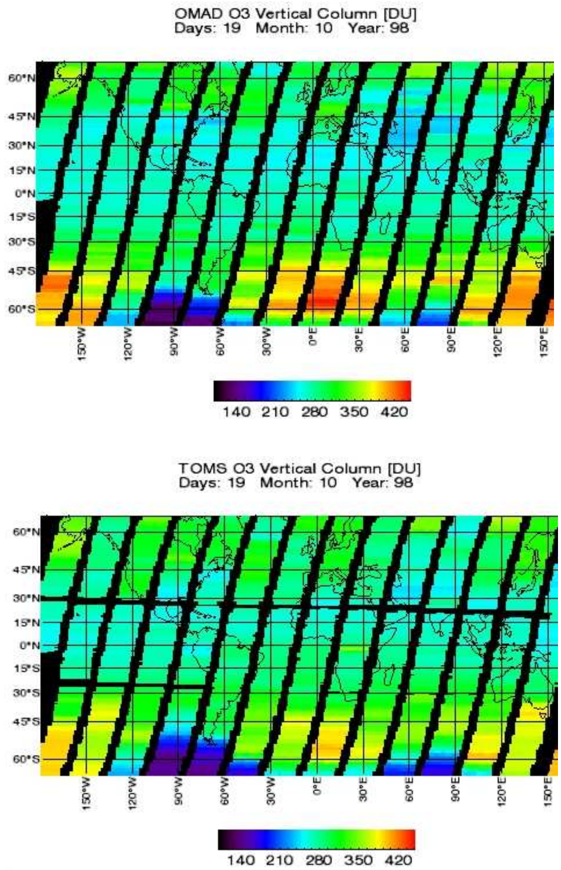

Figure 8: Total Ozone from OMAD and TOMS

Interestingly, cloud cover data derived from the OMAD and TOMS albedo (reflectivity) channels shows an even better correlation than that of the ozone products.

Monthly Average Total Ozone Content

OMAD data for October clearly shows the "ozone hole" over Antartica.

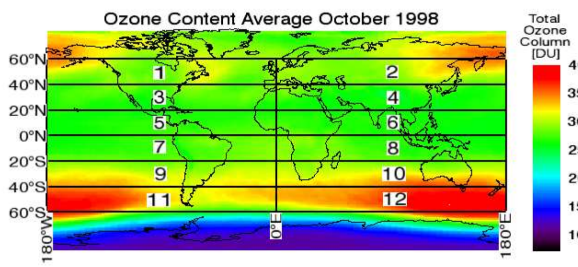

Figure 9: Ozone Monthly Total Ozone Average October 1998

CONCLUSIONS

A new analysis of OMAD data using an improved version of the simplified algorithm to find ozone content has been developed and tested. The potential of small satellites for atmospheric missions was discussed.

For the vertical column atmospheric content of ozone, multiple days were analysed over oceanic and continental masses using composites of up to 15 days, with ozone contents ranging from 150 DU to 400 DU.

Findings indicate a relative error between 5-15 % in the vertical column content of ozone given in Dobson Units (DU) as measured by OMAD with cross-correlations of the data between 0.65-0.9 when compared with NASA TOMS-Earth Probe data – depending on the geographical area from tropics to mid-latitudes in both hemispheres. This is considered to be good considering the low cost, mass and size of the OMAD.

FASat-Bravo has shown the potential for small satellites to act as atmospheric monitors.

Acknowledgments

The authors would like to thank NASA, SSTL and the many members of the FASat Project team, who worked so hard to make this mission a success. In particular we acknowledge the major contributions made by Alvaro Valenzuela, Marcelo Schoenherr, and Mario Arancibia of the Fuerza Aérea de Chile (FACH) to the original mission and instruments.

References

1. Underwood, C., Valenzuela, Alvaro., Schoenherr, Marcelo., Arancibia, Mario., Fouquet, Marc, *Initial in-orbit results from a low-cost atmospheric ozone monitor operating on board the FASat-Bravo microsatellite.* Phil. Trans. R. Soc. Lond, A, 2003. **361**: p. 71-76.

2. Fernandez-Saldivar, J.A., Underwood, C. I., Mackin, S. *Low-cost microsatellite UV instrument suite for monitoring ozone and volcanic sulphur dioxide*. in *Remote Sensing of Clouds and the Atmosphere XI.* 2006. Stockholm, Sweden: SPIE.